Electronic structure of epitaxial $(Sr,Ca)RuO_3$ films studied by photoemission and x-ray absorption spectroscopy

Jonghyurk Park* and Se-Jung Oh
School of Physics & Center for Strongly Correlated Materials Research, Seoul National University, Seoul 151-742, Korea

J.-H. Park
Department of Physics, Pohang University of Science and Technology, Pohang 790-784, Korea

D. M. Kim and C.-B. Eom
Department of Materials Science & Engineering, University of Wisconsin-Madison, Madison, Wisconsin 53706, USA
(Received 31 March 2003; published 25 February 2004)

Electronic structures of epitaxial $(Sr,Ca)RuO_3$ thin films are studied by photoemission and x-ray absorption spectroscopy using synchrotron radiation. The Ru $4d$ spectral weights obtained by utilizing the Cooper minimum phenomena of photoionization cross-section reveal a strong mixing between Ru $4d$ and O $2p$ states as well as the signature of electron correlation effect near the Fermi level in both $SrRuO_3$ and $CaRuO_3$. However the electron correlation effect seems more important in $CaRuO_3$ than $SrRuO_3$. The detailed shapes of the valence band are found to depend on the sample cleaning methods, where the single-crystalline films cleaned by *in situ* annealing show more enhanced structures in the spectra than the scraped polycrystalline samples.

DOI: 10.1103/PhysRevB.69.085108 PACS number(s): 71.30.+h, 78.70.Dm, 79.60.−i

I. INTRODUCTION

One of the central themes of the condensed-matter physics nowadays is the understanding of the electron correlation effects in solids. Motivated by the discovery of high-T_c superconductivity in cuprates and the colossal magnetoresistance effects in manganites, the research was initially focused on $3d$ transition-metal compounds. However, as it has become increasingly clear that interesting physical phenomena of similar origin also happen in $4d$ and $5d$ electron systems, they have been getting a fair amount of attention recently. Among the $4d$ or $5d$ transition-metal compounds, ruthenium oxides probably have attracted most attention because of the discovery of superconductivity in Sr_2RuO_4 (Ref. 1) and the potential of unique perovskite ferromagnetic metal $SrRuO_3$ (Ref. 2) for thin-film applications such as tunneling magnetoresistance or ferroelectric random access memory. These ruthenites also show diverse physical properties depending on the composition or crystal structures. For example, when Sr is replaced by Ca in the above ruthenates, the metallic and magnetic properties are significantly suppressed.[3,4] Ca_2RuO_4 is known as a Mott insulator, and $CaRuO_3$ is barely metallic with the low-temperature conductivity very close to the Mott minimum value. And the cubic pyrochlore structure $(Sr,Ca)_3Ru_2O_7$ system shows a typical bandwidth-controlled metal-insulator transition (MIT).[5,6] The Bi-based pyrochlore ruthenate is also well known to show MIT when doped with Y or rare-earth elements such as Gd or Nd.[7] And $Tl_2Ru_2O_7$ shows metal-insulator transition as a function of temperature.[8]

In this point of view, it is very natural to ask whether these critical phenomena can be described in terms of electron correlation effect in the same way as the $3d$ electron systems,[9–11] although $4d$ electrons of ruthenium oxides are more extended and the parent rutile RuO_2 is regarded as a good band metal. In the ternary ruthenium oxides, the Ru—O—Ru bonding angle turns out to considerably deviate from 180° due to tilting of the RuO_6 octahedron. For examples, the deviation of the bonding angle is as large as 8° in $SrRuO_3$ and increases to be twice in $CaRuO_3$, in spite of the fact that both perovskite ruthenates have a pseudocubic crystal structure. The deviation even becomes larger in the pyrochlore ruthenate. Thus the bandwidth of the Ru $4d$ stats is expected to be reduced accordingly, and the electron correlation may play a considerable role in their physical properties. In addition, recent spectroscopic studies suggest that some ruthenium oxides should be considered as strongly correlated electron systems. For example, $Ca_3Ru_2O_7$ can be thought of the typical Mott-insulator while $Sr_3Ru_2O_7$ is shown to be metallic from the high-resolution angle-resolved photoemission spectroscopy.[6] And, the recent optical spectroscopic study revealed that $SrRuO_3$ should be considered as a non-Fermi liquid system.[12–15] Ultraviolet photoemission data were also interpreted as indicating that Bi-based pyrochlore ruthenites $A_xB_{2-x}Ru_2O_7$ (A=Bi, B=Ln or Y) exhibit a systematic transition in the valence region from simple metallic to localized insulatorlike behavior.[3,16]

In this paper, we report the synchrotron-radiation photoemission (PES) and x-ray-absorption spectroscopy (XAS) data on the psuedocubic perovskite ruthenate epitaxial film $(Sr,Ca)RuO_3$ to study their electronic structures of both occupied and unoccupied states, focusing in particular on the role of the Ru $4d$ electronic states. In the case of $CaRuO_3$ only ultraviolet photoemission spectra of the valence band using He(I) source ($h\nu$=21.2 eV) has been reported[3(a)] previously to the authors' knowledge, and our work provides the first extensive electron spectroscopic studies of occupied and empty states using synchrotron radiation. For $SrRuO_3$ there have been two previous electron spectroscopic studies[17,18] using synchrotron radiation. But in these previous studies the Ru $4d$ partial spectral weights (PSW) were not determined separately, and also it turned out that our sample cleaning

procedure gave different spectra from those previously reported. Our data were taken from single-crystalline thin films of $SrRuO_3$ and $CaRuO_3$ grown epitaxially on the $SrTiO_3$ substrate, which were annealed *in situ* under oxygen pressure to obtain clean surfaces before PES and XAS measurements, while previous studies[17,18] used polycrystalline samples scraped *in situ*. Since scraping[19] tends to disrupt the surface region and our O $2p$ spectral weights are in much better agreement with band-structure calculations, we believe our spectra are more representative of the intrinsic valence band. We also obtained selectively the PSW of each element in the valence region by utilizing the large difference of the photoionization cross-sections between Ru $4d$ and O $2p$ orbitals depending on the incident photon energy due to the Cooper minimum phenomenon of Ru $4d$ states.[20,21] This enabled us to test in detail the validity of the theoretical partial density-of-states obtained from band-structure calculations. And we also report the x-ray absorption spectroscopy data at the O $1s$ edge to reveal the unoccupied electronic states of these ruthenium compounds.

II. EXPERIMENT

Epitaxial $Sr_{1-x}Ca_xRuO_3$ ($x=0$, 0.5, and 1) thin films were grown on miscut (001) SrTiO3 substrates using 90° off-axis sputtering.[22] And their surface morphology and crystal structure was confirmed to be single phase and stoichiometric in earlier surface-sensitive work by one of our authors. All the samples were found to be metallic from the transport measurement. We performed photoemission spectroscopy measurement on these single-crystalline films at various photon energies ranging from 40 to 100 eV at the beam line 2B1 of Pohang Light Source, Korea. The beam line was designed for the study of photoemission and magnetic circular dichroism, and the total experimental resolution was better than 0.2 eV. The base pressure during the photoemission measurement was in the middle of 10^{-10} torr range. As is well known, the photoemission spectroscopy is very sensitive to the surface condition of the sample, and we tried to clean the thin-film samples by moderately heating them ($T\sim450$ °C) *in situ* under the O_2 atmosphere of partial pressure 10^{-7} torr. We checked the cleanness of samples by surface-sensitive low-energy-electron-diffraction (LEED) and observed a clear (1×1) pattern of the (001) plane of the orthorhombic structure. The photoemission spectra were measured at the normal emission angle allowing a large acceptance solid angle, which corresponded to an angle-integrated density of states. The XAS experiment at the O $1s$ edge was carried out at the U4B beam line in National Synchrotron Light Source, Brookhaven National Laboratory, USA. The total yield (sample current) was measured, and the experimental resolution was better than 0.15 eV. All the spectroscopic measurements were performed at room temperature.

III. DATA AND RESULTS

Figures 1 and 2 show the photoemission spectra taken at various photon energies between 40 eV and 100 eV. All the spectra are normalized to the maximum peak intensity. We first note that the spectra of $SrRuO_3$ are somewhat different from the recently published data, where the spectra with the incident photon energy of $h\nu=48$, 52, and 100 eV were reported.[17] Our data show more structures between 3 eV and 8 eV binding energy compared with the previous data taken on scraped sample surfaces. Since similar structures were also seen in the previous He(I) ($h\nu=21.2$ eV) ultraviolet photoemission spectra on samples cleaned by annealing,[3] we believe this difference of the spectra results from the different sample cleaning methods (scraping versus annealing). The fact that these structures are predicted by band-structure calculations strongly suggests that annealed surfaces give the valence-band spectra more suitable for studying intrinsic electronic structures of these materials than scraped surfaces. By comparing our data with the density of states (DOS) from band-structure calculations,[26–28] we can assign two peaks

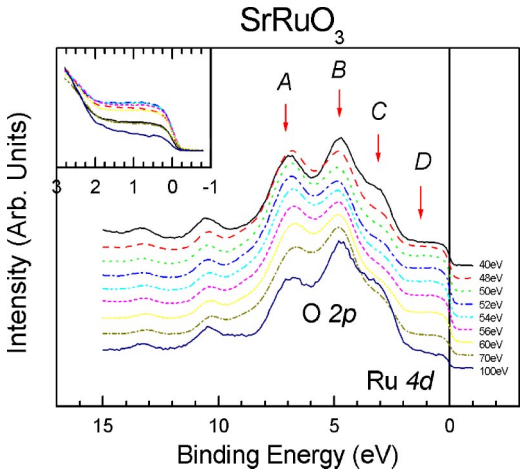

FIG. 1. (Color online) Valence-band spectra of $SrRuO_3$ taken at various photon energies from 40 eV to 100 eV, the same shown in inset.

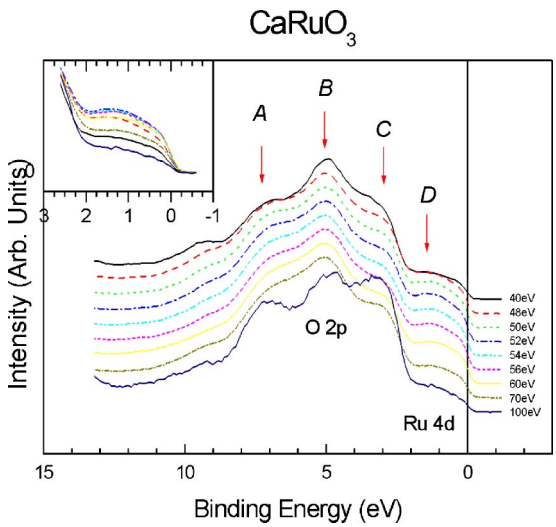

FIG. 2. (Color online) Valence-band spectra of $CaRuO_3$ taken at various photon energies from 40 eV to 100 eV, the same shown in inset.

(A,B) around 5–7 eV to O $2p$-derived bonding states and single peak (C) around 3 eV to nonbonding state of O $2p$ orbital. And Ru $4d$ t_{2g} state (D) mainly lies across the Fermi energy above O $2p$ state. The small peak around the binding energy of 10 eV is due to the contamination, most likely carbon monoxide. Although we did get the sharp LEED pattern through repeated annealing under O_2 atmosphere inside ultrahigh-vacuum (UHV) chamber, this feature could not be removed completely, as was also the case for scraped samples.[17] In our case some of this signal may have come from the sample holder due to the rather large incident photon beam, but it seems likely that this contamination is embedded in the sample itself. In both $SrRuO_3$ and $CaRuO_3$ spectra we can observe clear Fermi edges in the valence bands within the experimental resolution, in agreement with the transport data showing metallic behaviors.

The photoionization cross-section of Ru $4d$ electrons is well known to show strong dependence on the incident photon energy while that of O $2p$ electrons decreases monotonically as the photon energy increases.[23] Especially around 100 eV, the Ru $4d$ cross-section changes drastically and goes through a local minimum, the so-called "Cooper minimum."[20] In fact, such cross-section behaviors enable us to assign the peaks A–C to O $2p$-derived states and the peak D to Ru $4d$-derived states in Figs. 1 and 2. For example, the intensity ratio of the peak D relative to the peak C does not change much between 40 eV and 70 eV spectra, but is clearly reduced at 100 eV spectrum. Also this relative ratio between peaks D and C is quite small in all photon energy ranges, which agrees with the theoretical atomic cross-sections. The atomic calculation predicts that the relative photoionization cross-section of Ru $4d$ to O $2p$ orbitals is $\approx 2\%$ at $h\nu = 100$ eV. In solids, due to the hybridization between O $2p$ and Ru $4d$ orbitals, this value is somewhat changed and the Cooper minimum energy of Ru $4d$ orbital shifts toward higher energy.[21] However, making use of this energy dependence of the photoionization cross-sections we can derive separately the Ru $4d$ and O $2p$ PSW in the valence region, as will be shown in the following section.

Another interesting phenomenon such as Ru $4p \rightarrow 4d$ resonance, which was reported to occur around 52 eV,[17] can in principle also be utilized to deduce the PSW. However, the previous attempt in this direction was not quite successful partly because the resonance is not very strong compared with the cross-section variation of O $2p$ level and the valence region near Fermi energy is sensitive to the sample cleaning method. We also observed the moderate enhancement of the peak D relative to peak C around the photon energy of 50–60 eV as shown in the inset. Although this resonance effect was found to be rather broad and subtle compared with the well-known $3d \rightarrow 4f$ and $2p \rightarrow 3d$ cases, we obtained the strongest spectral intensity ratio of peaks D to C around the photon energy of 52–54 eV, which is consistent with the previous report.[17]

The O $1s$ XAS data of $Sr_{1-x}Ca_xRuO_3$ ($x=0$, 0.5 and 1) are shown in Fig. 3. We can see the systematic changes in the unoccupied Ru $4d$ state along with x. The sharp structure t_{2g} around 530 eV becomes somewhat smaller, and the rather broad feature e_g state around 531–535 eV splits into two narrower peaks as Sr is replaced by Ca. These two peaks come from the energy-level splitting of e_g state by the intra-atomic exchange interaction between $4d$ electrons whose magnitude is estimated to be about 1 eV, almost unchanged between samples. The e_g state has larger overlap with oxygen $2p$ state than t_{2g} in the pseudocubic symmetry. Therefore, the sharp t_{2g} state is more sensitive to the bonding angle than the broad e_g state. The Ru—O—Ru bonding angle in $CaRuO_3$ is much smaller than that in $SrRuO_3$ and lead to the less metallic behavior due to the smaller intensity of the t_{2g} peak. This change in unoccupied state is very consistent with the results in PES which will be discussed in the following section.

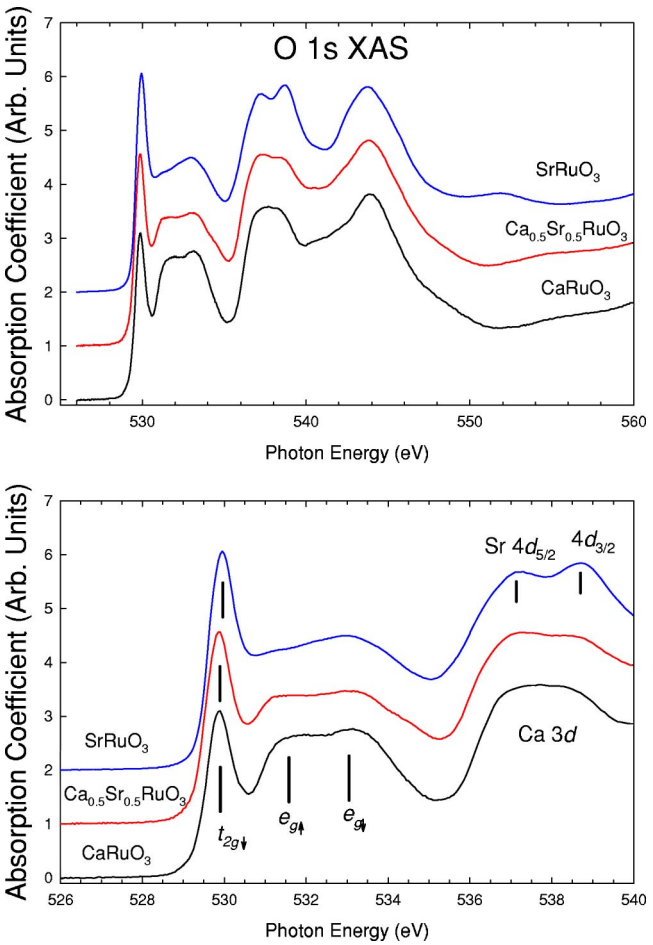

FIG. 3. (Color online) O $1s \rightarrow 2p$ x-ray absorption spectra of $(Sr,Ca)RuO_3$.

IV. DISCUSSION

To understand the electronic structures of $SrRuO_3$ and $CaRuO_3$, especially the role of electron correlations, it is important to extract PSW of Ru $4d$ and O $2p$ states separately and compare them with the band-structure calculations. For this purpose, we utilize the large difference of cross-sections depending on the incident photon energy in the following way. First, we regard the spectra around Cooper minimum of Ru $4d$ at the incident photon energy $h\nu = 100$ eV as the O $2p$ PSW, since theoretically the intensity

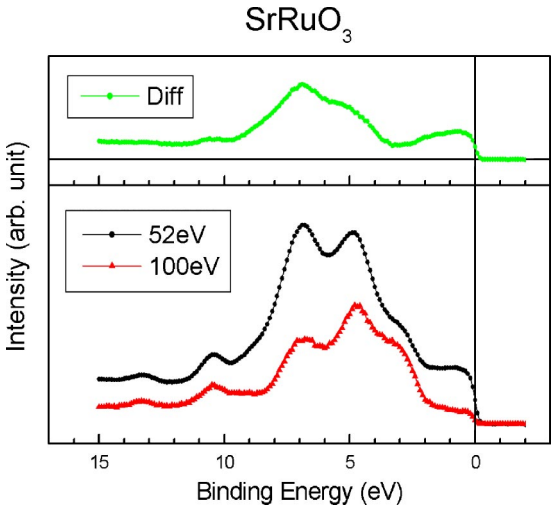

FIG. 4. (Color online) Method to obtain Ru $4d$ partial spectral weight of $SrRuO_3$.

ratio between Ru $4d$ and O $2p$ states should be negligible.[23] And then, Ru $4d$ PSW can be obtained by subtracting this spectrum from the one at lower photon energy where the Ru $4d$ contribution is large. We took $h\nu = 52$ eV spectrum for this purpose because around this energy Ru $4p \rightarrow 4d$ resonance occurs to enhance Ru $4d$ contributions. The results are shown in Figs. 4 and 5 for $SrRuO_3$ and $CaRuO_3$, respectively. The normalization was taken to make adventitious contamination peaks from carbon monoxide around ~ 10 eV, the same intensity to give almost flat spectral weight in this region. This procedure is reasonable since this peak arises from the bonding state 5σ of oxygen $2p$ and carbon $2s/2p$ orbitals in CO, whose photon energy dependence of the cross-section is similar to that of oxygen $2p$.[23–25]

To compare our experimental PSW's with theoretical band-structure calculations,[26–28] we removed inelastic backgrounds from the spectra in a way of the Shirley method.[29] Figures 6 and 7 show the resulting Ru $4d$ PSW and Figs. 8

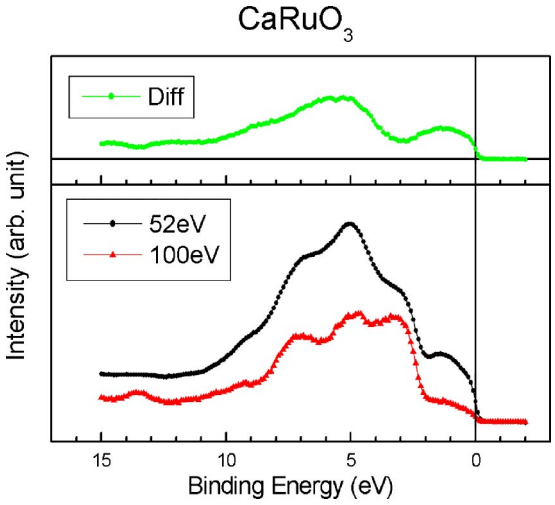

FIG. 5. (Color online) Method to obtain Ru $4d$ partial spectral weight of $CaRuO_3$.

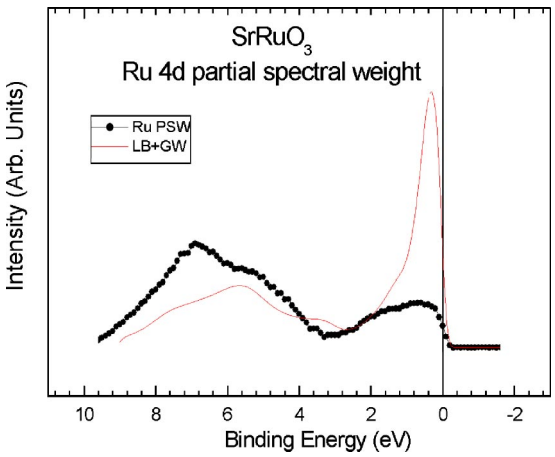

FIG. 6. (Color online) Comparison between experimentally deduced Ru $4d$ partial spectral weights of $SrRuO_3$ and the partial density of states from band-structure calculation (Ref. 27).

and 9 do the O $2p$ PSW for $SrRuO_3$ and $CaRuO_3$, respectively, in comparison with the corresponding theoretical partial DOS, which were the band calculation results[26,28] broadened with a convolution of the Gaussian and an energy-dependent Lorentzian functions. Gaussian width was set to 0.2 eV which was determined from the experimental resolution and Lorentzian width was fitted to a linear function of binding energy with no broadening at the Fermi level, simulating the lifetime broadening.

We can note a few things in the Ru $4d$ PSW shown in Figs. 6 and 7. First, Ru $4d$ states spread over a wide energy range, confirming very strong hybridization between Ru $4d$ and O $2p$ orbitals in these ruthenium compounds. This is consistent with the expectation that $4d$ orbital is quite extended and makes strong bonding, as predicted by the band-structure calculations. However, band calculation overemphasizes the spectral weights around the Fermi level in both $SrRuO_3$ and $CaRuO_3$. This apparent disagreement between band calculation and experimental PSW in regards to Ru $4d$

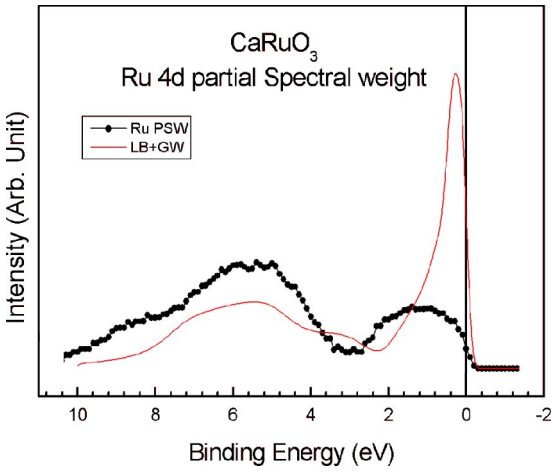

FIG. 7. (Color online) Comparison between experimentally deduced Ru $4d$ partial spectral weights of $CaRuO_3$ and the partial density-of-states from band-structure calculation (Ref. 28).

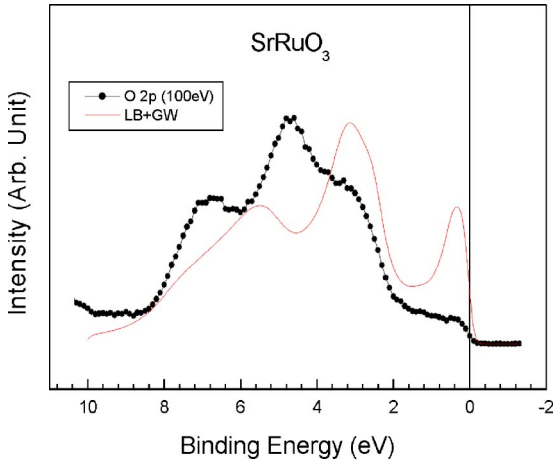

FIG. 8. (Color online) O $2p$ partial spectral weight of $SrRuO_3$ and its comparison with band-structure calculation (Ref. 27).

spectral weights around the Fermi level indicates the importance of electron correlation effect in the valence band. This disagreement might be attributed to the electron correlation effects which are neglected in the calculations. It is also pointed out in recent studies that the correlation energy of the Ru $4d$ electrons play an important role in physical behaviors, especially related to the states at the Fermi level, in the ternary ruthenium oxides.[6,15,30]

To address the correlation effect in the ruthenium compounds, the previous photoemission spectroscopic study[17] on $SrRuO_3$ assigned the Fermi-edge emission and the $\sim$1.2 eV peak to the coherent and the incoherent parts of the spectral function, respectively. They compared their data to the photoemission spectra of Ti and V oxides although the distinction between the two parts in the perovskite ruthenate case is less clear. Our data do not show a clear peak at $\sim$1.2 eV in $SrRuO_3$, and the detailed lineshape of the Ru $4d$ spectral weights near the Fermi level is found to depend sensitively on the methods of surface cleaning as in the $3d$ systems.[31,32] However, the comparison of the spectral weights near the Fermi level between $SrRuO_3$ and $CaRuO_3$ shown in Figs. 6 and 7 indicates the stronger reduction of the coherent peak and larger shift of spectral weights to the incoherent part in $CaRuO_3$. This change of the spectral weight between $SrRuO_3$ and $CaRuO_3$ is generally observed independent of the sample cleaning methods.[32] This fact implies that the electron correlation effect is stronger in $CaRuO_3$ than in $SrRuO_3$, consistent with the smaller effective mass in $SrRuO_3$ than in $CaRuO_3$ which explains the difference in the metallic property of the samples.

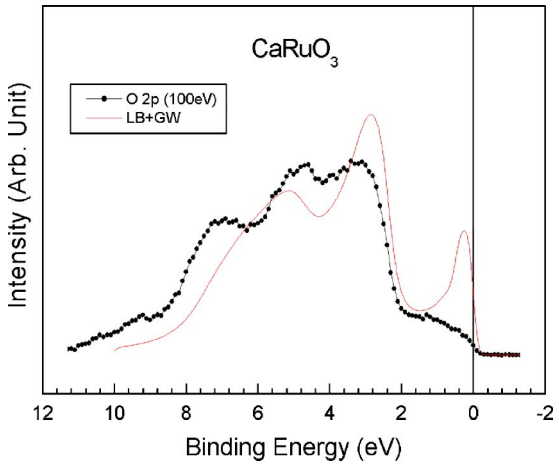

FIG. 9. (Color online) O $2p$ Partial spectral weight of $CaRuO_3$ and its comparison with band structure calculation (Ref. 28).

As for the O $2p$ spectral weights, we note that the three peak features shown in Figs. 8 and 9 are very similar to the previous report,[3] where they treated polycrystalline sample via *in situ* annealing under oxygen atmosphere to get the clean surfaces. These three peaks correspond to the O $2p$ nonbonding and the bonding states with Ru $4d$ levels. We can see that the O $2p$ nonbonding states around 3 eV are located at almost the same binding energy as the band theory calculation in both $SrRuO_3$ and $CaRuO_3$. In $CaRuO_3$, the overall features are quite consistent between theory and experiment for these oxygen-related features. In $SrRuO_3$, however, the bonding states have larger intensity than nonbonding state unlike the band calculation, and the binding energies are lower by about 0.8 eV. This probably indicates stronger hybridization effect between O $2p$ and Ru $4d$ states in $SrRuO_3$ compared with $CaRuO_3$. In both samples, the narrow Ru $4d$ feature near the Fermi level is much suppressed compared to the broad bonding states.

The O $1s$ XAS spectra shown in Fig. 3 are quite consistent with the above results of PES data. The prominent spectral changes of unoccupied state as Ca is substituted with Sr are (a) the decrease of the intensity of the sharp t_{2g} state and (b) the narrowing of the broad e_g states in $CaRuO_3$ compared with $SrRuO_3$. These effects come from the structural change leading to the substantial variation of the hybridization of Ru $4d$ with O $2p$ states and the localization of Ru $4d$ state in $CaRuO_3$. Although we could not observe the spectral transfer between coherent and incoherent states predicted in the Hubbard picture due to the strong O $1s$ core-hole effect, the localization effect of Ru $4d$ state is clearly shown and also supports our interpretation of the correlation effect between Ru $4d$ electrons.

V. CONCLUSION

We made a systematic study of electronic structures of ternary ruthenium oxides by photoemission and x-ray absorption spectroscopy. We obtained clean surfaces of $SrRuO_3$ and $CaRuO_3$ by *in situ* annealing of epitaxial thin films grown on $SrTiO_3$, and made use of strong dependence of the atomic cross-sections on the incident photon energy to obtain Ru $4d$ and O $2p$ PSW in the valence region. We confirmed a very strong hybridization between Ru $4d$ and O $2p$ states in both ruthenium compounds as predicted by band-structure calculation, but found that this one-electron hybridization effect alone cannot explain Ru $4d$ spectral weights near the Fermi level where the electron correlation effect seems to play a significant role. Our results are quite consistent with many studies which suggest the unique transport and magnetic properties of these ruthenates cannot

be explained by one-electron theory and the electron correlation should be taken into consideration in a similar way as the more strongly correlated $3d$ electron systems.

ACKNOWLEDGMENTS

This work is supported by the Korean Science and Engineering Foundation (KOSEF) through the Center for Strongly Correlated Materials Research (CSCMR) at Seoul National University and electron Spin Science Center (eSSC) at Pohang University of Science and Technology. The Pohang Light Source is supported by the Ministry of Science and Technology, Korea, and the work at NSLS is supported by the Department of Energy, US. The work at POSTECH is supported by Korea Research Foundation (Grant No. krf-2002-070-c00038) and POSTECH basic research fund. The work at UW-Madison was supported by the National Science Foundation under Grant No. DMR-9973801.

*Present address: Basic Research Laboratory, ETRI, Daejeon 305-350, Korea.

[1] Y. Maeno, H. Hashimoto, K. Yoshida, S. Nishizaki, T. Fujita, J.G. Bednorz, and F. Lichtenberg, Nature (London) **372**, 532 (1994).
[2] C.B. Eom, R.J. Cava, R.M. Fleming, J.M. Phillips, R.B. van Dover, J.H. Marshall, J.W.P. Hus, J.J. Krajewski, and W.F. Peck, Jr., Science **258**, 1766 (1992).
[3] P.A. Cox, R.G. Egdell, J.B. Goodenough, A. Hamnett, and C.C. Naish, J. Phys. C **16**, 6221 (1983), and references therein.
[4] M. Shepard, S. McCall, G. Cao, and J.E. Crow, J. Appl. Phys. **81**, 4978 (1997).
[5] S. Nakatsuji and Y. Maeno, Phys. Rev. Lett. **84**, 2666 (2000).
[6] A.V. Puchkov, M.C. Schabel, D.N. Basov, T. Startseva, G. Cao, T. Timusk, and Z.-X. Shen, Phys. Rev. Lett. **81**, 2747 (1998).
[7] S. Yoshii and M. Sato, J. Phys. Soc. Jpn. **68**, 3034 (1999).
[8] T. Takeda, M. Nagata, H. Kobayashi, R. Kanno, Y. Kawamot, M. Takano, T. Kamiyama, F. Izumi, and A.W. Sleight, J. Solid State Chem. **140**, 182 (1998).
[9] J.B. Goodenough, A. Hamnett, and D. Telles, in *Localization and Metal-Insulator Transition*, edited by H. Fritzsche and D. Adler (Plenum, New York 1985) p. 161.
[10] N.F. Mott, *Metal-Insulator Transisions* (Taylor & Francis Ltd., London, 1974).
[11] M. Imada, A. Fujimori, and Y. Tokura, Rev. Mod. Phys. **70**, 1039 (1998), and references therein.
[12] P. Kostic, Y. Okada, N.C. Collins, Z. Schlesinger, J.W. Reiner, L. Klein, A. Kapitulnik, T.H. Geballe, and M.R. Beasley, Phys. Rev. Lett. **81**, 2498 (1998).
[13] J.-S. Ahn, J. Bak, H.S. Choi, T.W. Noh, J.E. Han, Yunkyu Bang, J.H. Cho, and Q.X. Jia, Phys. Rev. Lett. **82**, 5321 (1999).
[14] J.S. Dodge, E. Kulatov, L. Klein, C.H. Ahn, J.W. Reiner, L. Mieville, T.H. Geballe, M.R. Beasley, A. Kapitulnik, H. Ohta, Yu. Uspenskii, and S. Halilov, Phys. Rev. B **60**, R6987 (1999).
[15] J.S. Dodge, C.P. Weber, J. Corson, J. Orenstein, Z. Schlesinger, J.W. Reiner, and M.R. Beasley, Phys. Rev. Lett. **85**, 4932 (2000).
[16] P.A. Cox, J.B. Goodenough, P.J. Taverner, and D. Telles, J. Solid State Chem. **62**, 360 (1986).
[17] K. Fujioka, J. Okamoto, T. Mizokawa, A. Fujimori, I. Hase, M. Abbate, H.J. Lin, C.T. Chen, Y. Takeda, and M. Takano, Phys. Rev. B **56**, 6380 (1997).
[18] J. Okamoto, T. Mizokawa, A. Fujimori, I. Hase, M. Nohara, H. Takagi, Y. Takeda, and M. Takano, Phys. Rev. B **60**, 2281 (1999).
[19] Scraping is widely used in UHV work to remove surface contamination, but, the exposed area of polycrystalline samples still contains large portion of grain boundary which is considered to significantly affect surface-sensitive spectroscopy study.
[20] U. Fano and J.W. Cooper, Rev. Mod. Phys. **40**, 441 (1968).
[21] I. Abbati, L. Braicovich, G. Rossi, I. Lindau, U. del Pennino, and S. Nannarone, Phys. Rev. Lett. **50**, 1799 (1983).
[22] Q. Gan, R.A. Rao, and C.B. Eom, Appl. Phys. Lett. **70**, 1962 (1997); R.A. Rao, Q. Gan, and C.B. Eom, *ibid.* **71**, 1171 (1997); C.B. Eom, R.A. Rao, Q. Gan, and D.B. Kacedon, J. Appl. Phys. **83**, 6539 (1998).
[23] J.J. Yeh and I. Lindau, At. Data Nucl. Data Tables **32**, 1 (1984).
[24] l. Wilhelmy, L. Ackermann, A. Garling, and N. Rösch, J. Chem. Phys. **100**, 2808 (1994).
[25] E.W. Plummer, T. Gustafsson, W. Gudat, and D.E. Eastman, Phys. Rev. A **15**, 2339 (1977).
[26] P.B. Allen, H. Berger, O. Chauvet, L. Forro, T. Jarlborg, A. Junod, B. Revaz, and G. Santi, Phys. Rev. B **53**, 4393 (1996).
[27] D. Singh, J. Appl. Phys. **79**, 4818 (1996).
[28] I.I. Mazin, and D.J. Singh, Phys. Rev. B **56**, 2556 (1997).
[29] D.A. Shirley, Phys. Rev. B **5**, 4709 (1972).
[30] J.S. Lee, Y.S. Lee, T.W. Noh, K. Char, Jonghyurk Park, S.-J. Oh, J.-H. Park, C.B. Eom, T. Takeda and R. Kanno, Phys. Rev. B **64**, 245107 (2001).
[31] Y. Aiura, H. Kawanaka, H. Bando, and T. Yasue, J. Vac. Sci. Technol. A **19**, 1929 (2001).
[32] J. H. Kim, Y. D. Zhao, J. Chung, and S.-J. Oh (unpublished).